ISSN 0915-633X

# NATIONAL INSTITUTE FOR FUSION SCIENCE

## Observations and Modelling of Line Intensity Ratios of OV Multiplet Lines for $2s3s\ ^3S_1$ - $2s3p\ ^3Pj$

T. Kato, E. Rachlew-Källne, P. Hörling and K.-D Zastrow

(Received - July 16, 1996 )

NIFS-436 Aug. 1996

RESEARCH REPORT
NIFS Series



NAGOYA, JAPAN

# Observations and modelling of line intensity ratios of OV multiplet lines for 2s3s $^3S_1$ - 2s3p $^3P_J$.

T. Kato[1], E. Rachlew-Källne, P. Hörling and K.-D. Zastrow[2]

*Department of Physics I. Royal Institute of Technology (KTH). S-10044 Stockholm, Sweden*

[1] *National Institute for Fusion Science, Nagoya 464-01, Japan*

[2] *JET Joint Undertaking, Abingdon OX14 3EA, England*

(August 26, 1996)

## Abstract

Line intensity ratios of OV multiplet lines for the 2s3s $^3S_1$ - 2s3p $^3P_J$ ($J$=2,1,0) transitions are studied using a collisional radiative model and the results are compared with measurements from the reversed field pinch experiments Extrap T1 and T2 at KTH. The measured line intensity ratios deviate from the predictions from the model and the possible causes for the discrepancy are discussed with regard to errors in rate coefficients and non quasi steady state.



Keywords;

O V ion, line intensity ratio, multiplet lines, collisional radiative model

## 1. INTRODUCTION

The triplet lines 2s3s $^3S_1$- 2s3p $^3P_{2,1,0}$ of Be-like OV ions are frequently used in plasma diagnostics since the line intensities are strong and the wavelengths are in the UV - visible range (2781.04 Å, 2787.03 Åand 2789.86 Å). The lines are often used for ion temperature measurements through measurements of the Doppler broadened line profiles. However, also the line intensity ratios are of diagnostic interest since they are temperature and density sensitive in regions of interest for plasma diagnostics. It has previously been observed that these line ratios do not agree with those predicted by the statistical weights of the J states in the multiplet. Furthermore, measurements of lifetimes (Engström et al 1981) have shown that the multiplet lines show different lifetimes due to a J-selective transition in the multiplet. We have constructed a collisional radiative model for OV with fine structure levels and studied the line intensity ratios for density and temperature diagnostics (Kato et al, 1990). In this paper the calculated electron density and temperature dependences of the line ratios of these multiplet lines are compared with measurements from the Extrap T1 and T2 RFP experiments.

Be-like ions have the metastable state 2s2p $^3P^0_{2,1,0}$. Since the radiative decay rate is zero for the level 2s2p $^3P^0_0$, the population density of the metastable state is not negligible even at low electron densities. Consequently, the population of the excited states are affected by the metastable state also at low plasma densities. For example, excitation from the metastable state 2s2p $^3P^0_0$ contributes 50 percent to the population of 2s3p $^3P^0_0$ in the low density limit.

The OV multiplet is an interesting example for testing atomic data in a collisional radiative model since several plasma laboratory experiments at different conditions and with different time scales have shown the line ratios to deviate from the values expected from Boltzmann distributions including transition rates and statistical weights. In particular, laboratory experiments with very different time scales are of interest since these observations could give information on which processes are important for the population and decay of the states involved. The existence of metastable states is of interest since these states are

populated in the plasma and their influence on the line intensities is important when modelling the radiation processes from the plasma. Recently, experiments from a small tokamak (Kallstenius, 1994) have shown the same non-statistical multiplet line intensity ratios and these deviations were interpreted as caused by polarisation effects.

## 2. ATOMIC DATA

The energies for the 20 fine structure levels in the n= 2 and 3 ($2s^2$, 2s2p, $2p^2$, 2s3s, 2s3p, 2s3d) configurations of OV are taken from Moore (1980). Fig. 1 shows a level diagram of the levels included in the calculations. The data for transition probabilities between n=2 and n=3 levels are taken from Hibbert (1980). The electron excitation rate coefficients are taken from the fitted data in the analytical formula given by Kato et al (1990) which are based on the data by Berrington (1987). We also include the excitation by protons with data from Doyle et al(1987) for the fine structure transitions within the triplet 2s2p $^3P^o$ and $2p^2$ $^3P$ levels. Proton excitation is important in high temperature ($T_e \geq 100$ eV) and low density ($n_e \leq 10^{12}$ $cm^{-3}$) plasmas (Kato et al, 1990).

Recently, Csanak et al (1996) calculated the excitation cross sections by the distorted wave method for the transitions $2s^2$- 2s2p, $2p^2$, 2s3s, 2s2p - 2s3p and 2s3s - 2s3d, 2s3p for magnetic sublevels. We have compared these data with those of Kato et al (1990). The comparison of the excitation rate coefficients is shown in Fig.2. The data by Csanak et al (1996) are sometimes lower than those of Kato et al (1990). The differences at low temperatures might be due to resonances which are not taken into account in the data by Csanak et al (1996). However, for the rate coefficients with values larger than $10^{-10}$ $cm^3s^{-1}$ the agreement is within 20 percent.

## 3. COLLISIONAL RADIATIVE MODEL OF OV WITH FINE STRUCTURE LEVELS

The 20 fine structure levels of $2s^2$, 2s2p, $2p^2$, 2s3s, 2s3p, 2s3d are included in our model (see Fig.1). The temperature and density dependences for some line intensity ratios of OV are given in Kato et al (1990).

### a) Metastable state 2s2p $^3P_J$

Be-like ions have the metastable state 2s2p $^3P^0_J$. The transition probability $A_r$ for radiative decay from the metastable state to the ground state $2s^2(^1S)$ is very small: $A_r(2\ ^3P^0_1 - 2\ ^1S_0) = 2.17\text{x}10^3\ s^{-1}$, $A_r(2\ ^3P^0_2 - 2\ ^1S_0) = 2.16\text{x}10^{-2}\ s^{-1}$ and $A_r(2\ ^3P^0_0 - 2\ ^1S_0) = 0\ s^{-1}$ (Hibbert, 1990). Since the value $A_r(2\ ^3P^0_0 - 2\ ^1S_0) = 0$, the population of the 2s2p $^3P^0_0$ is not zero even in the low density limit. Therefore the population of the excited states is affected by the metastable state even in low density plasmas. Excitation from the metastable state 2s2p $^3P^0_0$ contributes 50 percent to the population of the 2s3p $^3P^0_0$ state in the low density limit. Population of the 2s2p $^3P^0_2$ and 2s2p $^3P^0_1$ states begins to affect the 2s3p $^3P^0_0$ state at densities of $10^5$ and $10^{10}$ $cm^{-3}$, respectively. The excitation from $2p^2\ ^3P_J$ and the cascade from 2s3d $^3D_J$ become dominant for the population of 2s3p $^3P^0_J$ from $10^{15}$ and $10^{16}$ $cm^{-3}$, respectively. The deexcitation from 2s2p $^1P^0$ to 2s2p $^3P^0_J$ becomes effective for $n_e \geq 10^{16}$ $cm^{-3}$.

Our model in this paper includes all the fine structure levels (LSJ levels) up to n = 3 (fine structure model). However, generally the population densities are obtained by taking into account LS levels such as 2s2p $^3P$ as a single level and taking the average transition probability for the three fine structure levels $J$ = 0,1,2. We call this case a combined level model here. The results of the calculated population with the fine structure level model and the combined level model, respectively, are different due to the different values of the radiative transition probabilities, $A_r$, in the case of the fine structure model and the combined

level model. Therefore, we would like to point out that the population of the 2s2p $^3$P by the combined level model and by the sum of the fine structure model $\Sigma J$ n(2s2p $^3P_J$) are not the same.

The reduced population densities n(i)/[n(1)g(i)] for the 2s2p $^3P^0_J$ are shown in Fig. 3(a) where n(i) and g(i) are the population density and the statistical weight of the excited state i. The reduced population density of 2s2p $^3P^0_J$ and of 2p$^2$ $^3P_J$ in Fig. 3(a) have the same value for different J values for $n_e \geq 10^{12}$ cm$^{-1}$; the population densities with different J in the same configuration 2s2p $^3$P or 2p$^2$ $^3$P reach the ratio of the statistical weight. In Fig.3 (b) n(i)/n(1)/g(i)/$n_e$, which is the reduced population density divided by the electron density $n_e$ for 2s3p $^3P^0_J$, is shown. The population densities of 2s3p $^3P^0_J$ are not in the statistical ratios as shown in Fig.3 (b). The population density ratios reach the statistical ratio for $n_e \geq 10^{15}$ cm$^{-3}$ for $T_e$ = 30 eV. However in the case of $T_e$ = 100 eV, the population ratio changes at around $10^{14}$ cm$^{-3}$; the reduced population density of 2s3p $^3P^0_0$ is the largest among the levels of the 2s3p configuration for $n_e \leq 10^{14}$ cm$^{-3}$ whereas the 2s3p $^3P^0_2$ is the largest for $n_e \geq 10^{14}$ cm$^{-3}$. This might be due to the excitation from 2s3p $^3P_J$ to 2s3d $^3D_J$. The excitation rate coefficients from 2s3p $^3P_0$ are larger than those from 2s3p $^3P_2$ by 50 percent at 30 eV and 80 percent at 100 eV. For $n_e = 10^{17}$ - $10^{18}$, the reduced population density of 2s3p $^3P_0$ again becomes the most abundant. The population density ratios reach the statistical ratio for $n_e \geq 10^{18}$ cm$^{-3}$. This is due to the excitation rate coefficients between the fine structure levels in 2s3p $^3P_J$. The maximum deviation from the statistical ratio at $n_e \geq 10^{14}$ is 15 percent at $n_e = 10^{17}$ for $T_e$ = 100 eV.

**b). Line intensity ratios**

The calculated normalized line intensities divided by $n_e$ for the multiplet lines I = n(i)$A_r$(i→j)/$\Sigma$n(i)$n_e$ are shown in Figs. 4 (a) and (b) as a function of the $T_e$ and $n_e$, respectively. As seen in Fig. 4, the temperature dependence is a sensitive function of $n_e$, an

effect which becomes strong at temperatures higher than 100 eV. The density dependence is not so strong below $T_e$ = 100 eV. The normalized line intensities decrease rapidly for $n_e \geq 10^{14}$ cm$^{-3}$ which means that the population of the 2s3p levels reaches a nearly constant value for increasing $n_e$. The calculated line intensity ratios are shown in Fig. 5 as a function of electron densities for $T_e$ = 30 eV and 100 eV. The solid lines indicate the results with the excitation data given in Kato et al (1990) and the dotted ones with the data by Csanak et al (1996). The difference is small, to within a few percent. The temperature dependences of the intensity ratios are weak as shown in Fig. 6. As we have seen in Fig. 5, the line intensity ratios between 2s3s $^3S_1$ - 2s3p $^3P^0_{2,1,0}$ transitions do not follow what could be expected from the statistical weights of the levels at densities below $n_e \leq 10^{18}$ cm$^{-3}$.

## 4. EXPERIMENTAL OBSERVATIONS

The spectral line intensities of the multiplets 2s3s $^3S_1$ - 2s3p $^3P^0_J$, 2781.04Å(J=2), 2787.03Å(J=1), 2789.86Å(J=0) have been measured from the Extrap T1 and T2 reversed field pinch experiments at KTH. The Extrap-T1 experiment (Mazur et al, 1994) is a small-size toroidal plasma with a major radius of 0.5 m and a minor radius of 0.057 m and is equipped with a stainless-steel vacuum liner. Typical discharge times are between 400 — 700 $\mu$s with $n_e$ = 0.5 - 1.5.10$^{14}$ cm$^{-3}$ and $T_e$ = 150 - 275 eV. The discharges were normally performed using hydrogen as filling gas, and oxygen was the most common impurity with concentrations of several percent. The Extrap-T2 reversed-field pinch (Brunsell et al, 1995) is a larger toroidal device (major radius 1.5 m, minor radius 0.19 m) with carbon tiles as plasma facing surface. Discharge times up to 15 ms are obtained with $n_e$ = 0.2 - 1.0.10$^{14}$ cm$^{-3}$, $T_e$ = 50 - 200 eV. The ion temperatures are found to be approximately equal to the electron temperatures. The OV multiplet studied here was the brightest one in the visible and near-UV wavelength region in both devices during the central and hottest period of the discharges. A typical spectrum of the OV multiplet is shown in Fig. 7. The light was

collected with a single line-of-sight along a diameter in a poloidal plane of the torus using a 600 $\mu$m diameter quartz fiber. A 1-m focal length Czerny-Turner monochromator equipped with a 2400 l/mm grating and a gateable, 1024 pixel intensified multichannel detector was used (gated typically for 30 - 100 $\mu$s).

The spectra were fitted with a nonlinear least square fitting routine (Hörling et al, 1995). The high line intensities resulted in very good fits giving small error bars to the fits. To investigate the error due to count statistics, OV spectra were simulated with the typical noise characteristics of the detector and for different intensities of the lines (Hörling et al, 1995). For the typical multiplet line intensities of 1-2 x $10^4$ counts this resulted in line ratio errors of 2-3 percent for the two line ratios considered here.

The spread of the fitted line ratios for the data sets of 75 similar plasma discharges from the EXTRAP-T2 are shown in Fig. 8. The double standard deviation of the mean ($2\sigma_\mu$) obtained are 0.014, 0.062 respectively. This means an error in the line ratio measurements for one data point of 0.5 - 1 percent.

To be able to conclude that the observed line ratios are free from systematic errors the following three checks were made:

i) The spectral region around the multiplet was searched for other known impurities. No lines, forming multiplets which should have a strong component blended with any of the OV lines were found. This method can be used assuming the J substates of a state being populated according to its statistical weight factors. Then the resulting line intensities of a multiplet can be estimated, knowing only the intensity of a single member line. Blending with metal lines could be a problem in the Extrap-T1, but they were normally weak, and absent in Extrap-T2.

ii) The variation of the sensitivity of the system over the three OV lines (spanning 8 Å) could have some impact on the measurement. No calibration lamp with known spectral radiance around 2785 Å was available. However, studying the continuum light (radiative recombination radiation) in the initial plasma breakdown phase, no strong sensitivity deviations was seen over the detector channel range. Above 3000 Å, using a tungsten calibration

lamp, the variation of sensitivity was negligible over the part of the photodiode array onto which the OV lines were focussed. Variations of the attenuation of the port window at the experiment, the fiber and lenses used should be very small over only 10 Å but, if significant, give an opposite effect than the one we see namely that the lowest wavelength line is too strong (attenuation increases with decreasing wavelength).

iii) The electron density and temperature varies along the line-of-sight in a pinch plasma, as does the density and emissivity distributions of ions. These variations are, however, not large enough to have a significant influence on the result, because the OV ions are not supposed to be abundant in the cooler and less dense edge region of the plasma where the gradients of $T_e$ and $n_e$ might be large.

The peak value of the electron temperature $T_e$ is about 100 - 300 eV and the electron density is about $5x10^{13}$ - $10^{14}$ $cm^{-3}$. The observed mean ratios of I(J=2)/I(J=0) and I(J=1)/I(J=0) are 5.75 ± 0.15 and 2.95 ± 0.10, respectively as seen from Fig. 8.

It should also be remarked that this RFP experiment is not sensitive to any possible polarisation effects since the single line-of-sight crosses through the plasma with the direction of the magnetic field varying strongly along the line-of-sight and the electron velocity distribution is expected to be isotropic.

## 5. COMPARISON WITH MEASUREMENTS

The observed line intensity ratios are consistent with the predictions only if the OV lines are emitted from a plasma of $T_e$ = 200 eV and $n_e \geq 10^{15}$ $cm^{-3}$ as shown in Figs. 5 and 6.

The problem is that this high electron density is needed to bring consistency with theoretical predictions and measurements and such high electron densities are inconsistent with other measurements of the electron density in the plasma. It should also be noted that the small errors in the line ratio measurements, as discussed previously, should make the measurements sensitive enough to see the variations predicted by the model. However, the

discrepancy with the theoretical prediction in the line ratio measurement is well beyond the statistical experimental error and indicates a systematic difference of too small line ratio values predicted from the model.

As is seen from Fig. 5, the measured intensity ratio of I(J=2)/I(J'=0) is larger than the theoretical calculation for the relevant plasma parameters ($T_e \sim 250$ eV, $n_e \sim 7.10^{13}$ $cm^{-3}$) by 12 percent whereas the experimental error is 2-3 percent. However, the calculated ratio of I(J=1)/I(J'=0) is almost in the experimental error. This indicates that the measured intensity I(J=2) is significantly larger than the results from the calculation compared to those of I(J=1) and I(J=0).

## 6. DISCUSSION

The measurements do not agree with the theoretical calculations. We consider here the contribution of ionisation and recombination. The effect of ionisation from the excited state on the intensity ratios is smaller than 5 percent, although the effect on the population density is much larger than 5 percent. This effect for the higher levels is effective at lower temperatures since the ionisation potential is lower for the higher levels. We assume the density of the Li-like and B-like ions to be the same as the Be-like ions to see the effect. It should also be emphasized that this assumption is supported by line intensity measurements in the VUV region of the oxygen lines.

### a) Inner sub-shell ionisation

From the ground state of B-like ions $2s^2 2p\ ^2P$ the metastable state $2s2p\ ^3P^0$ of Be-like ions is easily produced via inner sub-shell ionisation processes. We have previously studied the effect of ionisation in Kato et al (1990). This effect is larger for the triplet lines than for the singlet lines. When the population of the metastable state is increased through inner

sub-shell ionisation, the excitation rate to the 2s3p $^3P^0$ will increase. We have included inner sub-shell ionisation from B-like ground state to the 2s2p $^3P^0$ levels. The rate coefficients are assumed according to the statistical weights of the final states. This assumption is considered to be reasonable from the data by Sampson and Zhang (1988) for the inner shell ionisation process from Li-like to He-like ions, such as $1s^22s + e \rightarrow 1s2s + 2e$, if the population density of the ground doublet state of B-like ions ($2s^22p\ ^2P_{1/2,3/2}$) is populated according to the statistical ratio. The population densities are increased effectively for $T_e \geq 100$ eV but the line ratios are not changed.

**b) Electron recombination**

When the lines are emitted near the edge of the plasma where the electron temperature is low recombination might be important. The total recombination rate coefficient at 30 eV is $2x10^{-11}$ $cm^3s^{-1}$. The effective emission rate coefficient for electron excitation of the weakest multiplet line at $n_e = 10^{14}$ $cm^{-3}$ is $5x10^{-11}$ and $1x10^{-10}$ $cm^3s^{-1}$ for 30 eV and 100 eV, respectively. The partial recombination rate coefficients to the 2s3p $^3P^0$ levels are estimated to be of the order of $10^{-16}$ $cm^3s^{-1}$ which is very small and the major part of the recombination comes through cascade from higher levels. Therefore, we have to know the density effect of the dielectronic recombination rate around $10^{14}$ $cm^{-3}$. The thermal limit at $T_e = 30$ - 100 eV and $n_e = 10^{13}$ - $10^{14}$ $cm^{-3}$ is about n = 8 - 11. The recombination rate is estimated to be only 2 - 5 percent for this plasma condition. Then the recombination rate is about $(4\text{-}10)x10^{-13}$ $cm^3s^{-1}$. This value is small compared to the excitation rate coefficient. Therefore, it is necessary to include a density of Li-like ions about 100 times that of the Be-like ions which is not realistic. Furthermore, since the recombination rates are so small the time for this process is too long in the RFP plasma discharges with densities $10^{13}$ - $10^{14}$ $cm^{-3}$ and particle confinement times of 20 - 40 $\mu$s (typical values for the EXTRAP-T1 plasma). This even further emphasizes that the ionisation processes are completely dominating the

population of the levels involved in the observed transitions.

### c) Proton collisions

We have included proton excitation between fine structure levels in the 2s2p state as well as in the $2p^2$ state but not in the 2s3p state. In order to see the effect of the proton collisions, we have added the proton excitation for 2s3p $^3P^0$ levels assuming the same excitation rate coefficients for 2s2p $^3P^0$. But this effect is small and no difference was found. In Fig. 5 the line ratio of I(J=2)/I(J'=0) and I(J=1)/I(J'=0) increases for $n_e \geq 10^{14}$ cm$^{-3}$. The reason for this increase could be due to the competition between the radiative decay from 2s3p $^3P$ and collisions from 2s3p $^3P^0$. The reduced population density n(i)/g(i) of 2s3p $^3P^0_2$ is larger than those of J=0 and 1 in the density region of $10^{14}$ - $10^{16}$ cm$^{-3}$ at $T_e$ = 100 eV.

### d) Cascade from 2s3d $^3$D

The cascade contribution from 2s3d $^3$D to 2s3p $^3P^0$ state becomes important for $n_e \geq 10^{14}$ cm$^{-3}$ in our calculation. However, if the population of the 2s3d $^3D_J$ state is according to the statistical ratio, the population of the 2s3p $^3P^0$ is also in the statistical ratio. We can not reproduce the line ratio I(J=2)/I(J'=0) greater than 5 through cascades. But the important factor is the competition between the collisional process and the radiative process. We have decreased the rate coefficients from 2s2p $^3P$ to 2s3p $^3P$ by 20 percent. The ratios are very sensitive to these rate coefficients. However, we can not reproduce the ratio larger than 5 by decreasing the rate coefficients.

### e) Non quasi steady state effect

In laboratory plasmas, such as in the divertor plasmas, the plasma is not ionisation

equilibrium but generally in an ionising state due to the diffusion and recycling. In order to know the line intensities in such ionising plasmas, we generally solve the time dependent rate equations of the ions taking into account the ionisation and recombination between the ground states and after that we calculate the line intensities corresponding to the abundance of each ion; this is called the quasi steady state assumption. In our calculation we assumed a quasi steady state dn(i)/dt = 0 for the population of the plasma. However, the metastable state 2s3p $^3$P has a long decay time and remains in the plasma and we have to solve the time dependent rate equations for the population of the metastable states relative to the ground state (Kato et al 1996). Therefore, this effect will change the population of 2s3p $^3P_J$ which is mainly produced by excitation from 2s2p $^3P_J$.

## 7. CONCLUSIONS

We have discussed the possible origin of the disagreement between the measurements and the theoretical calculations for the OV multiplet. We can exclude any influence of electron recombination and proton collisions while the rate coefficients might still be in error. We conclude, however, that the most probable sources are the assumption of the quasi steady state and the error of the rate coefficients. The non quasi steady state requires a time dependent rate equation including the metastable states. These results are of significance for the general application of steady state collisional radiative models.

## ACKNOWLEDGEMENTS

This research has been supported by the European Communities under an association contract between EURATOM and the Swedish Natural Science Research Council (NFR). Support from the Göran Gustafsson Foundation is also gratefully acknowledged. We would also like to thank Prof. T. Fujimoto and Prof. J. Dubau for useful comments and discussions

and the Los Alamos group (Drs. G. Csanak, R. Clark and J. Abdallah) for communicating their data prior to publication.

## REFERENCES

Berrington K.A., 1987, private communication

Brunsell P. et al, 1995, 22nd European conf. on Contr. Fusion and Plasma Physics, III-157

Csanak G., Clark R. and Abdallah J., to be published, 1996

Doyle J.G., Kingston A.E. and Reid R.H., 1987, Astron. Astrophys. **90**, 97

Engström L. et al, 1981, Physica Scripta **24** 551

Hibbert A., 1980, J. Phys. **B13**, 1721

Hörling P. and Zastrow K.-D., 1995, J. Quant. Spectr. Rad. Transfer **53**, 585

Kallstenius T, 1994, MSc thesis, Royal Institute of Technology (KTH), TRITA-FYS-1034, ISSN 0280-316X

Kato T., Lang J. and Berrington K.A., 1990, Atomic Data and Nucl. Data Tables **44** 133

Kato T., Moribayashi K., Murakami I., Ohira M., Kubo H. and Shimizu K., 1996, to be published in Fusion Engineering and Design

Mazur S., Nordlund P., Zastrow K.-D. Brzozowski J.H. and Drake J.R., 1994, Nucl. Fusion **34**, 427

Moore C.E., 1980, NSRDS-NBS 3, Sect.9

Sampson D. H. and Zhang H.L., 1988, Phys. Rev. A **37**, 3765

## Figure Captions

Fig. 1. Level diagram of the levels included in the calculation. On the bars are printed the number of the type of the configuration and within parenthesis the number of fine structure levels (in total 20). The transition studied is shown with a dashed line.

Fig. 2. Comparison of excitation rate coefficients (F) from Kato et al (1990) and Csanak et al (1996) a) shows F(2s2p $^3P_0^0$- 2s3p $^3P_0^0$), b) F(2s2p $^3P_0^0$ - 2s3p $^3P_1^0$), c) F(2s2p $^3P_0^0$ - 2s3p $^3P_2^0$) and d) F(2s2p $^3P_1^0$ - 2s3p $^3P_0^0$).

Fig. 3. Reduced population density of OV ions at $T_e$ = 30 eV.

a) n(i)/ n(1)/ g(i) where n(i) and g(i) is the population density and the statistical weight of level i.

b) n(i)/ n(1)/ g(i)/ $n_e$ for the level 2s3p $^3P_{2,1,0}^0$

Fig. 4. The multiplet line intensities for OV as a function of

a) the electron temperature, $T_e$ and b) the electron density, $n_e$

Fig. 5. The line intensity ratios of I(2781(J=2))/I(2789(J=0)) and I(2787(J=1))/ I(2789(J=0)). Observed values are shown by arrows.

Fig. 6. The line intensity ratios as a function of the electron temperature $T_e$.

Fig. 7. A spectrum with fit of the OV multiplet obtained from Extrap-T2 (Shot# 1499).

Fig. 8. The spread of the measured line intensity ratios for a data set of 75 similar discharges in EXTRAP. The vertical arrows show the ratios computed theoretically from the typical plasma operating point $T_e$ = 250 eV, $n_e = 7.10^{13}$ cm$^{-13}$. The horizontal bars to the right of the histogram represents the fit error due to count statistics.

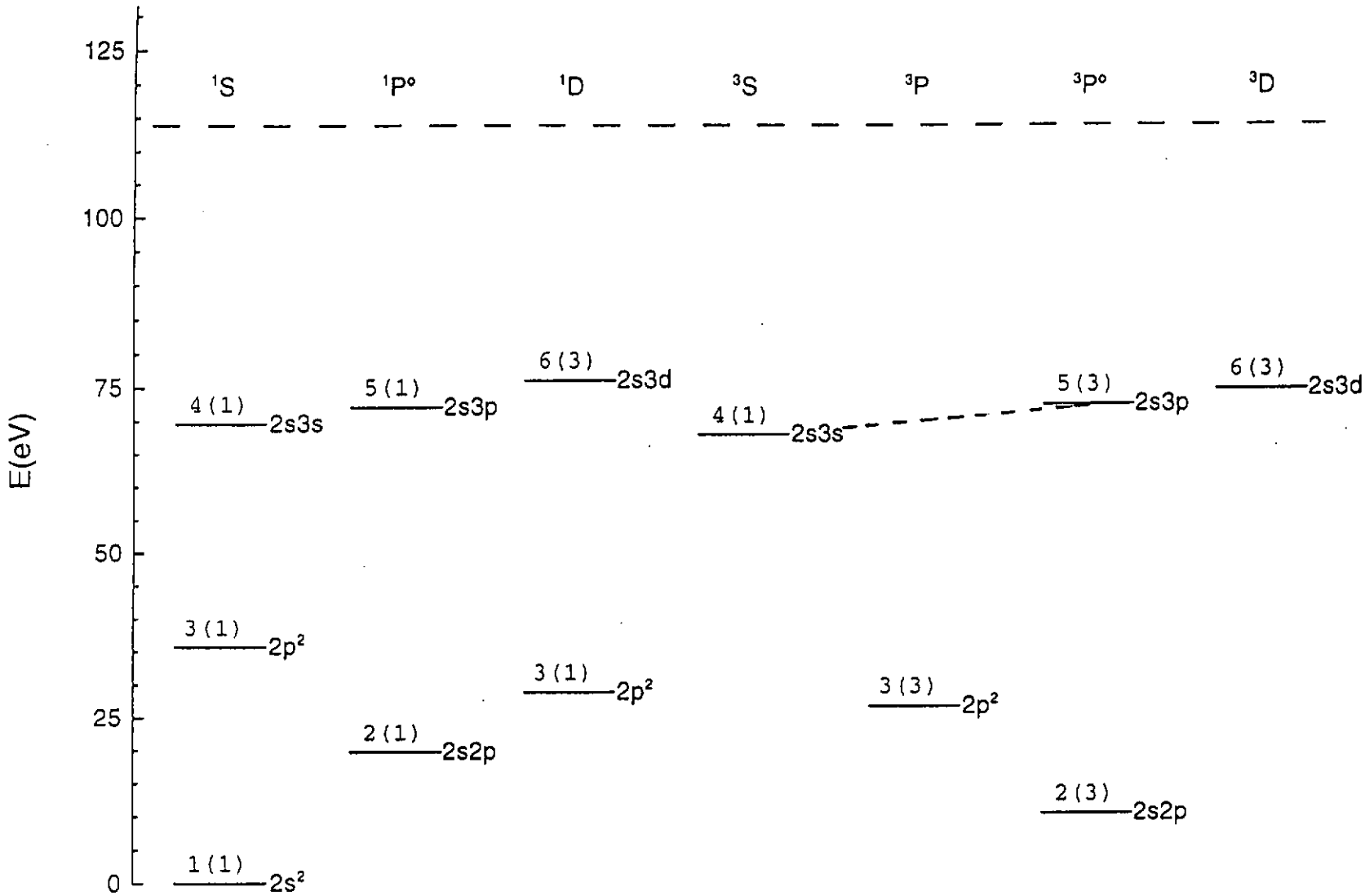
E(eV)
125
100
75
50
25
0
1S
1P°
1D
3S
3P
3P°
3D
4 (1) 2s3s
5 (1) 2s3p
6 (3) 2s3d
4 (1) 2s3s
5 (3) 2s3p
6 (3) 2s3d
3 (1) 2p²
2 (1) 2s2p
3 (1) 2p²
3 (3) 2p²
2 (3) 2s2p
1 (1) 2s²

Fig. 1

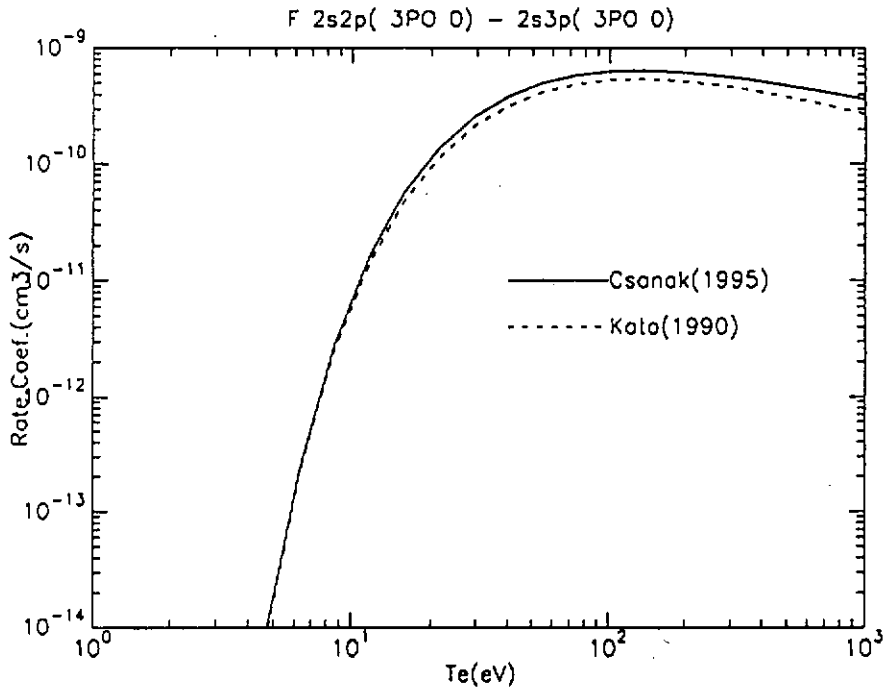
F 2s2p( 3PO 0) - 2s3p( 3PO 0)
Rate_Coef.(cm3/s)
Te(eV)
Csanak(1995)
Kato(1990)

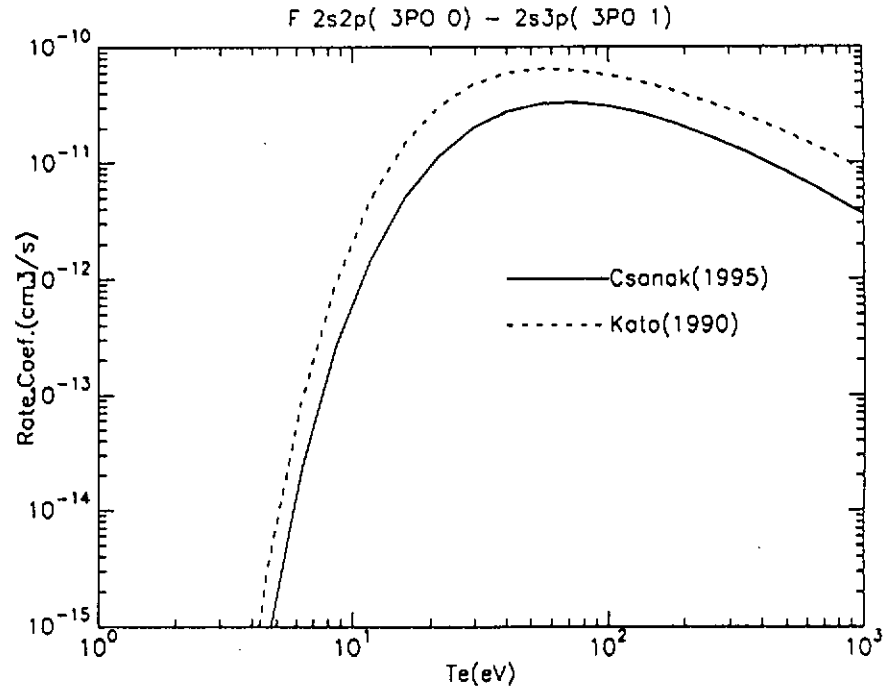
F 2s2p( 3PO 0) - 2s3p( 3PO 1)
Rate_Coef.(cm3/s)
Te(eV)
Csanak(1995)
Kato(1990)

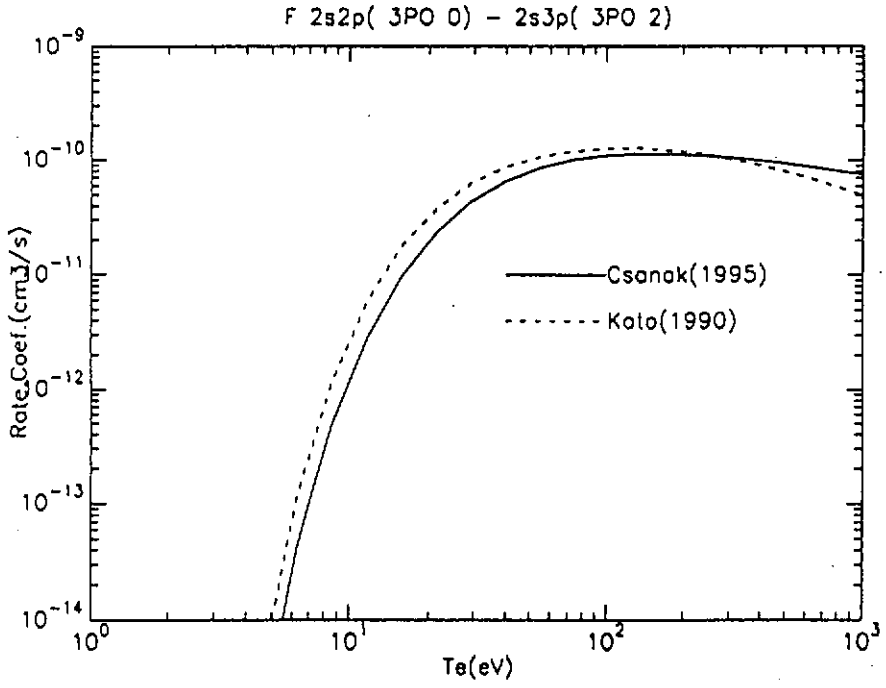
F 2s2p( 3PO 0) - 2s3p( 3PO 2)
Rate_Coef.(cm3/s)
Te(eV)
Csanak(1995)
Kato(1990)

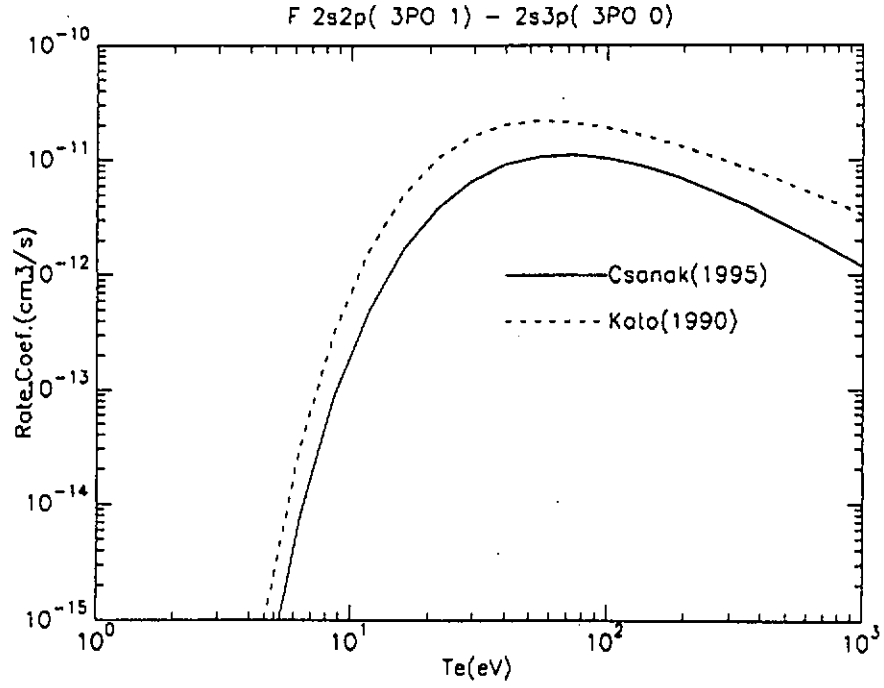
F 2s2p( 3PO 1) - 2s3p( 3PO 0)
Rate_Coef.(cm3/s)
Te(eV)
Csanak(1995)
Kato(1990)

Fig.2

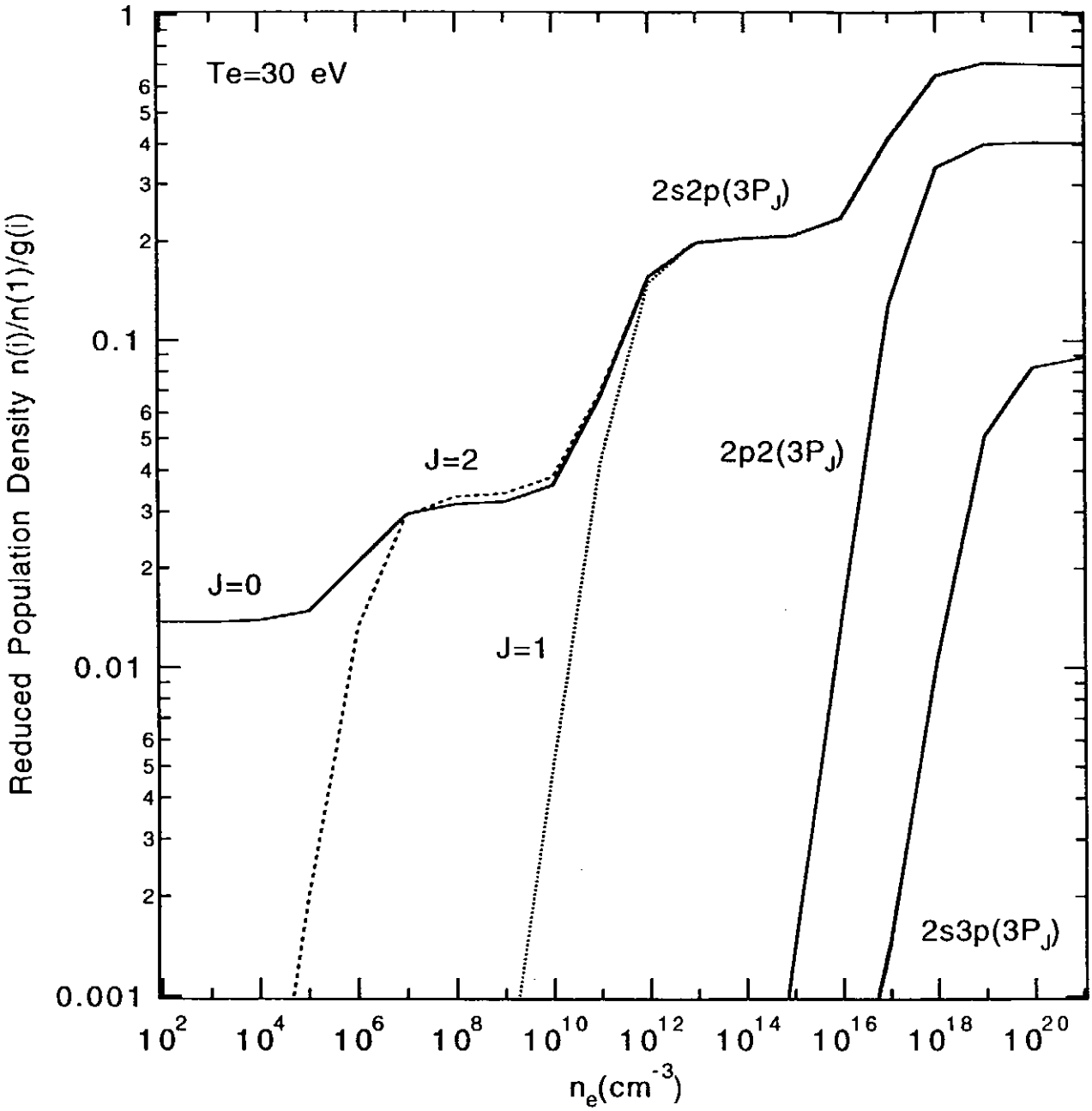
Te=30 eV
2s2p(3P_J)
2p2(3P_J)
2s3p(3P_J)
J=2
J=0
J=1
Reduced Population Density n(i)/n(1)/g(i)
n_e(cm^-3)
1
0.1
0.01
0.001
10^2
10^4
10^6
10^8
10^10
10^12
10^14
10^16
10^18
10^20

Fig.3(a)

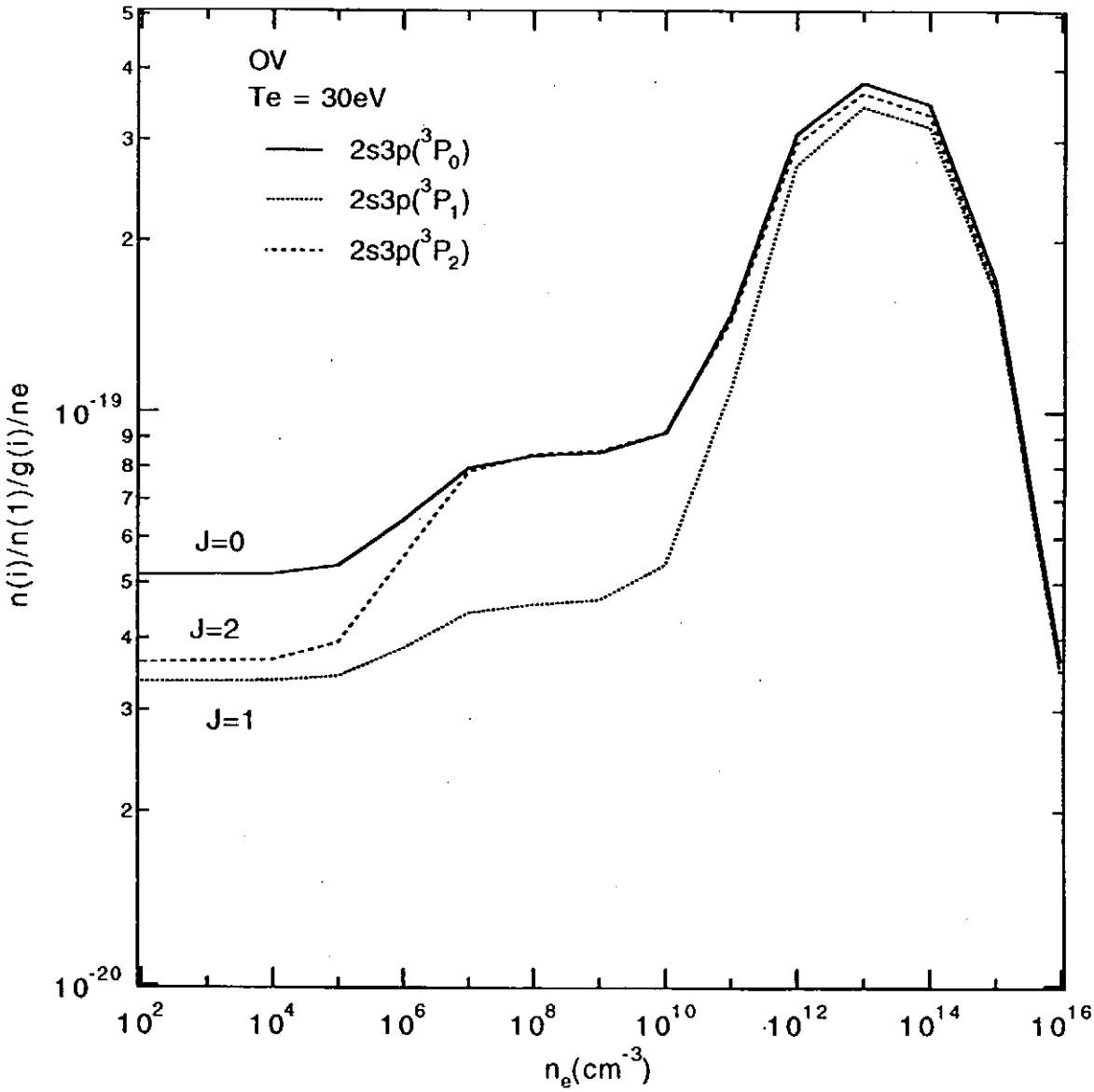


Fig.3(b)

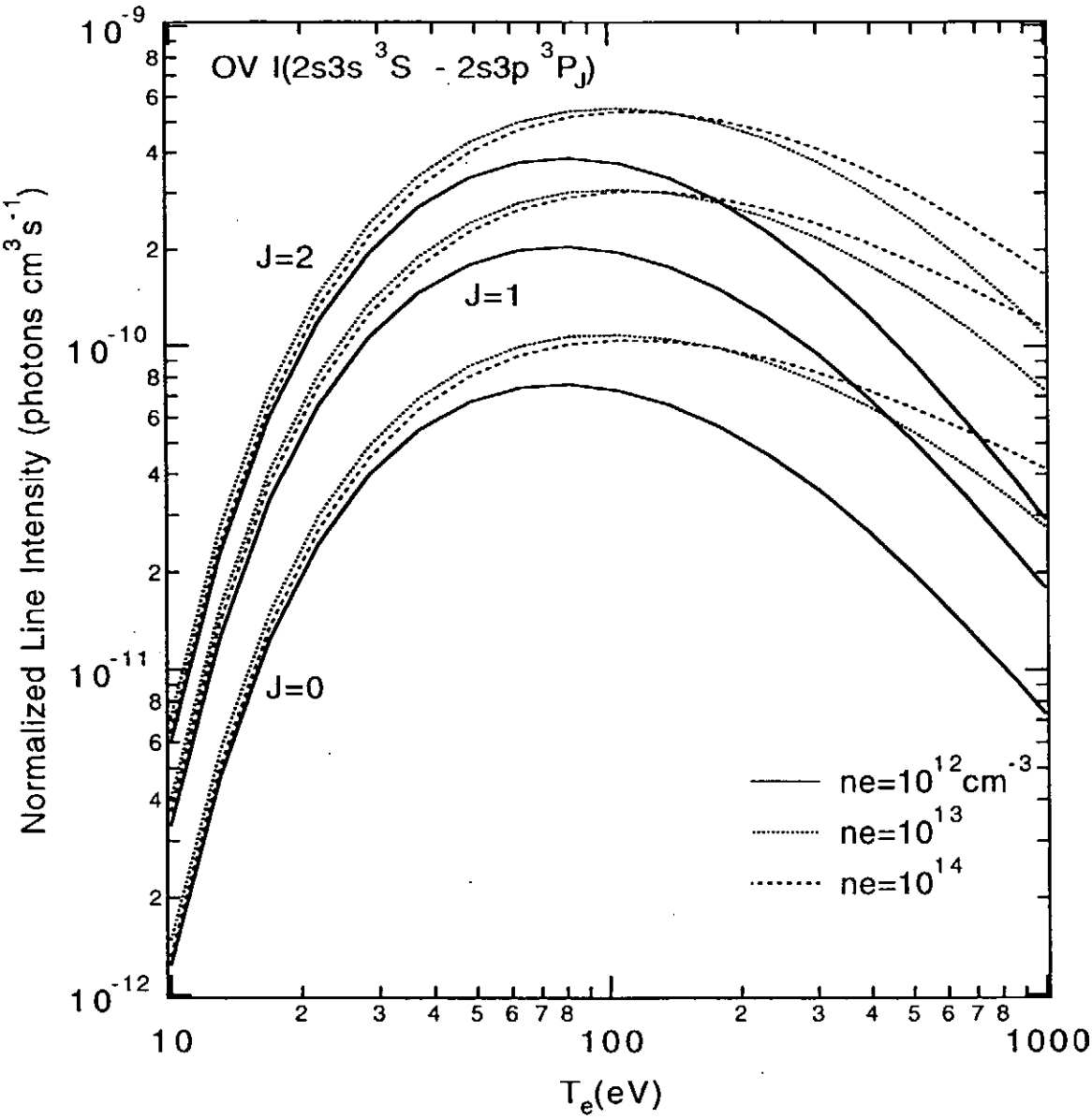
OV I(2s3s $^3$S - 2s3p $^3$P$_J$)
Normalized Line Intensity (photons cm$^3$ s$^{-1}$)
$10^{-9}$
$10^{-10}$
$10^{-11}$
$10^{-12}$
J=2
J=1
J=0
ne=$10^{12}$cm$^{-3}$
ne=$10^{13}$
ne=$10^{14}$
10
100
1000
$T_e$(eV)

Fig.4(a)

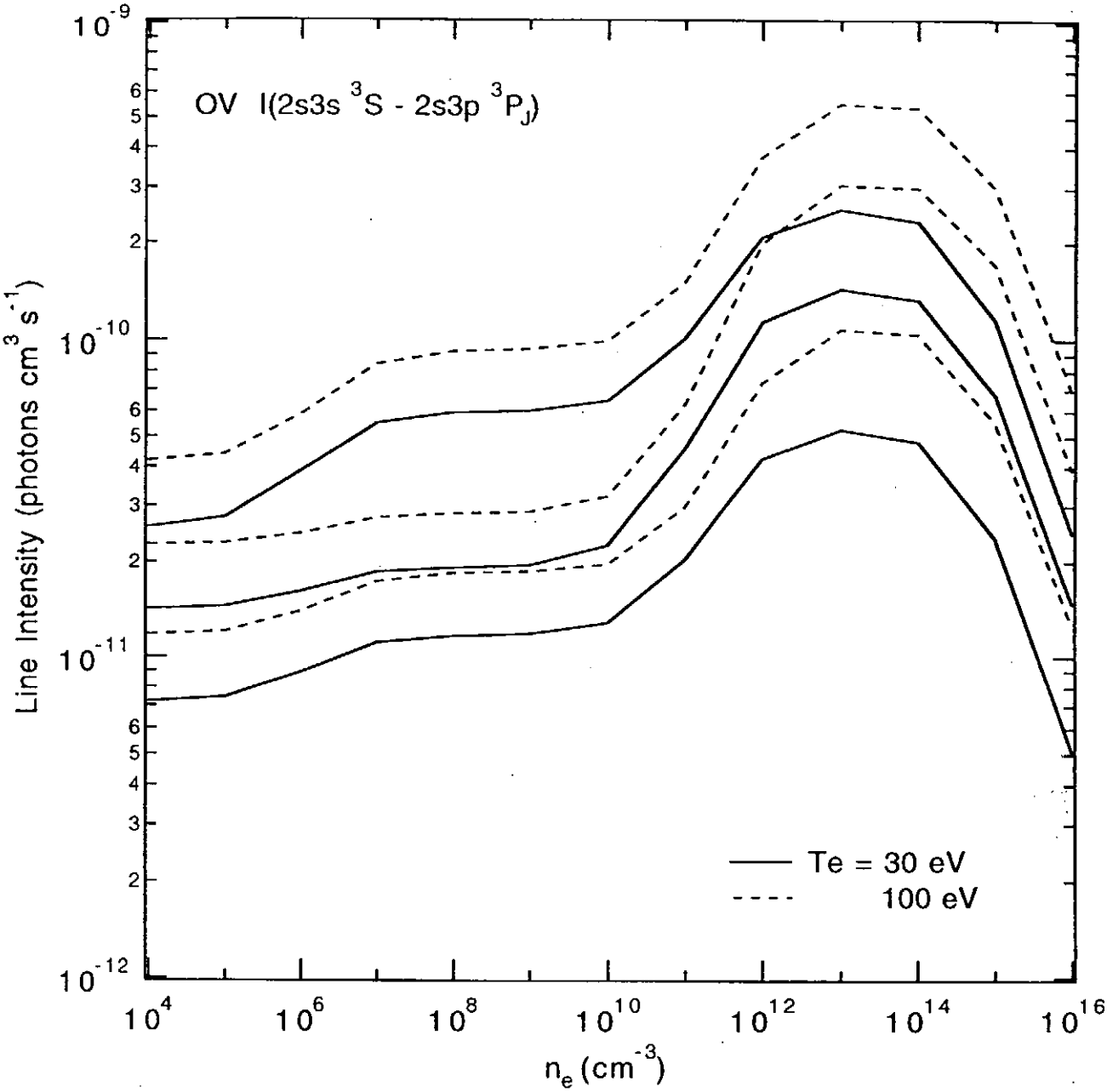
OV I(2s3s $^3$S - 2s3p $^3$P$_J$)
Line Intensity (photons cm$^3$ s$^{-1}$)
$10^{-9}$
$10^{-10}$
$10^{-11}$
$10^{-12}$
$10^4$
$10^6$
$10^8$
$10^{10}$
$10^{12}$
$10^{14}$
$10^{16}$
$n_e$ (cm$^{-3}$)
Te = 30 eV
100 eV

Fig.4(b)

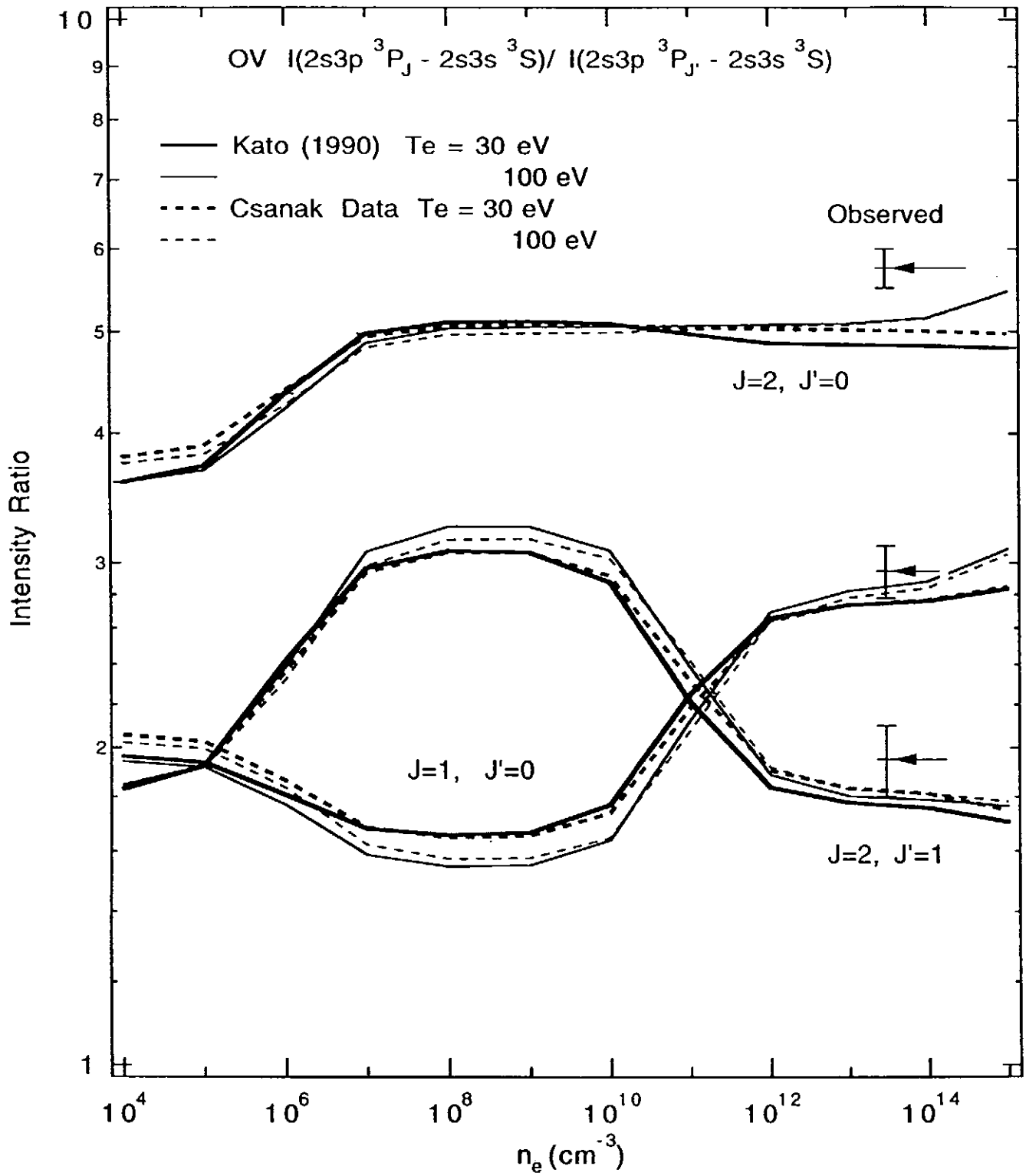
OV I(2s3p $^3P_J$ - 2s3s $^3S$)/ I(2s3p $^3P_{J'}$ - 2s3s $^3S$)
Kato (1990) Te = 30 eV
100 eV
Csanak Data Te = 30 eV
100 eV
Observed
J=2, J'=0
J=1, J'=0
J=2, J'=1
Intensity Ratio
$n_e$ ($cm^{-3}$)
10
9
8
7
6
5
4
3
2
1
$10^4$
$10^6$
$10^8$
$10^{10}$
$10^{12}$
$10^{14}$

Fig.5

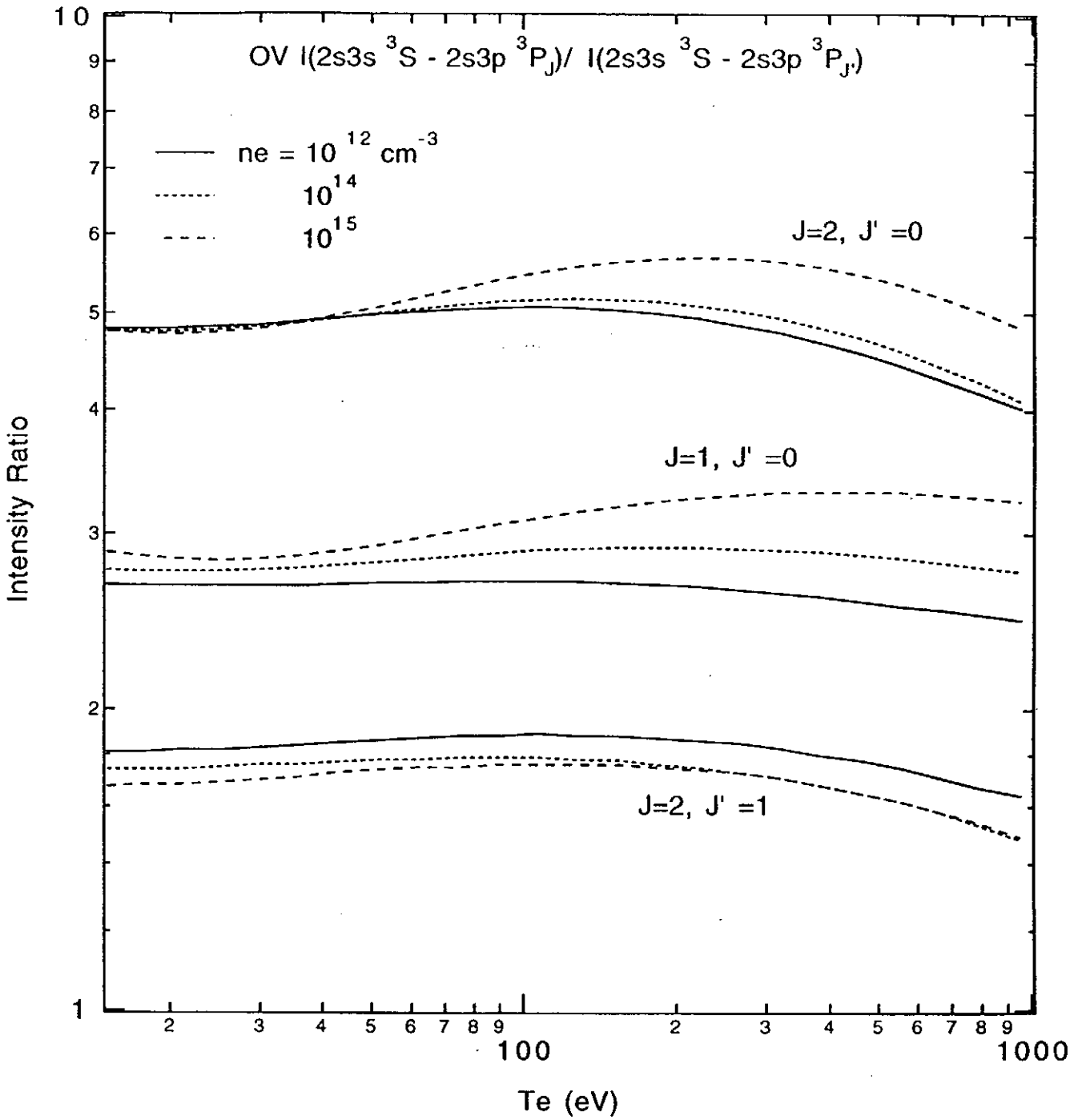
OV I(2s3s $^3$S - 2s3p $^3$P$_J$)/ I(2s3s $^3$S - 2s3p $^3$P$_{J'}$)
ne = 10$^{12}$ cm$^{-3}$
10$^{14}$
10$^{15}$
J=2, J' =0
J=1, J' =0
J=2, J' =1
Intensity Ratio
Te (eV)
10
9
8
7
6
5
4
3
2
1
2 3 4 5 6 7 8 9
100
2 3 4 5 6 7 8 9
1000

Fig.6

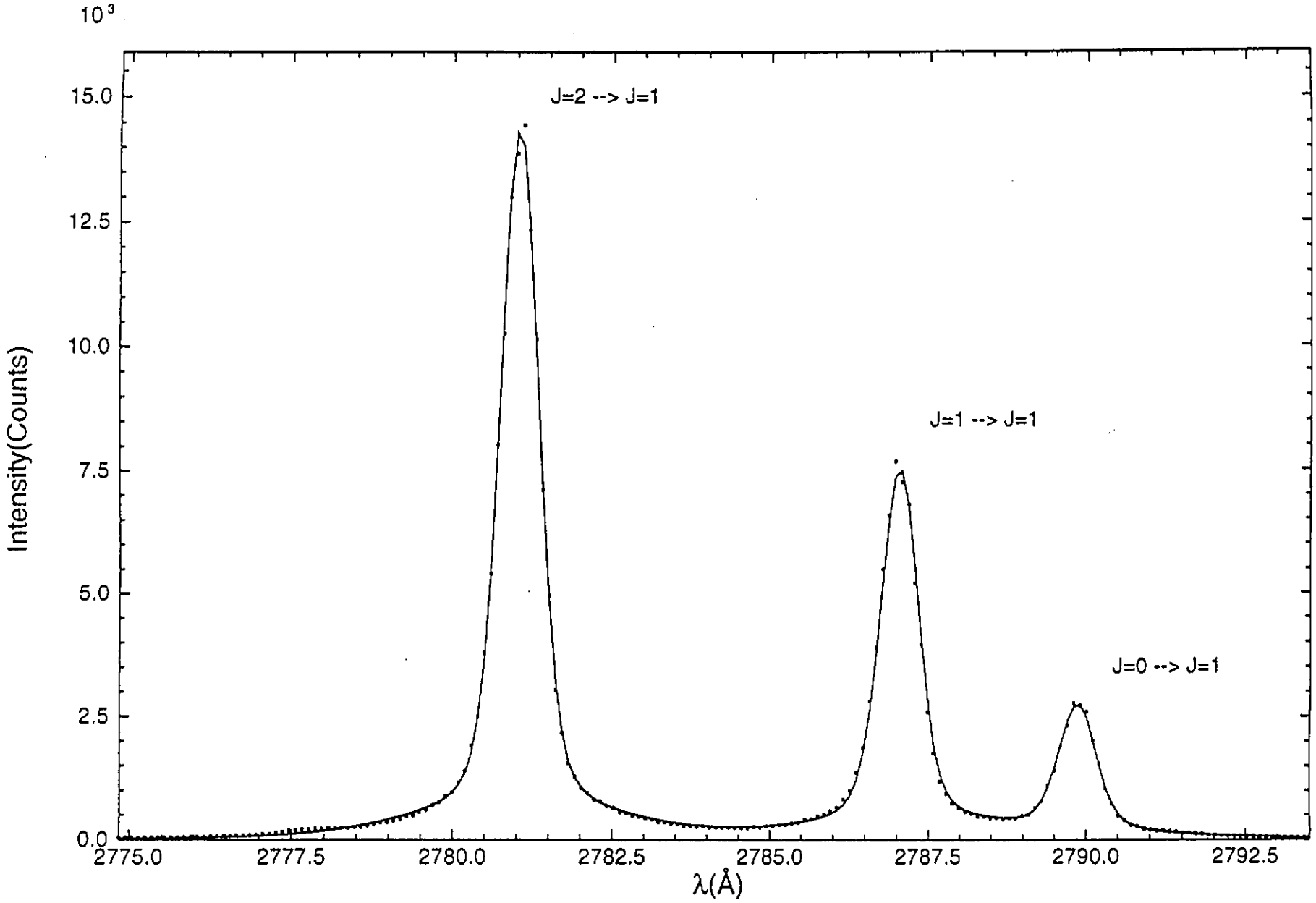
10³
15.0
12.5
10.0
7.5
5.0
2.5
0.0
Intensity(Counts)
J=2 --> J=1
J=1 --> J=1
J=0 --> J=1
2775.0
2777.5
2780.0
2782.5
2785.0
2787.5
2790.0
2792.5
λ(Å)

Fig.7

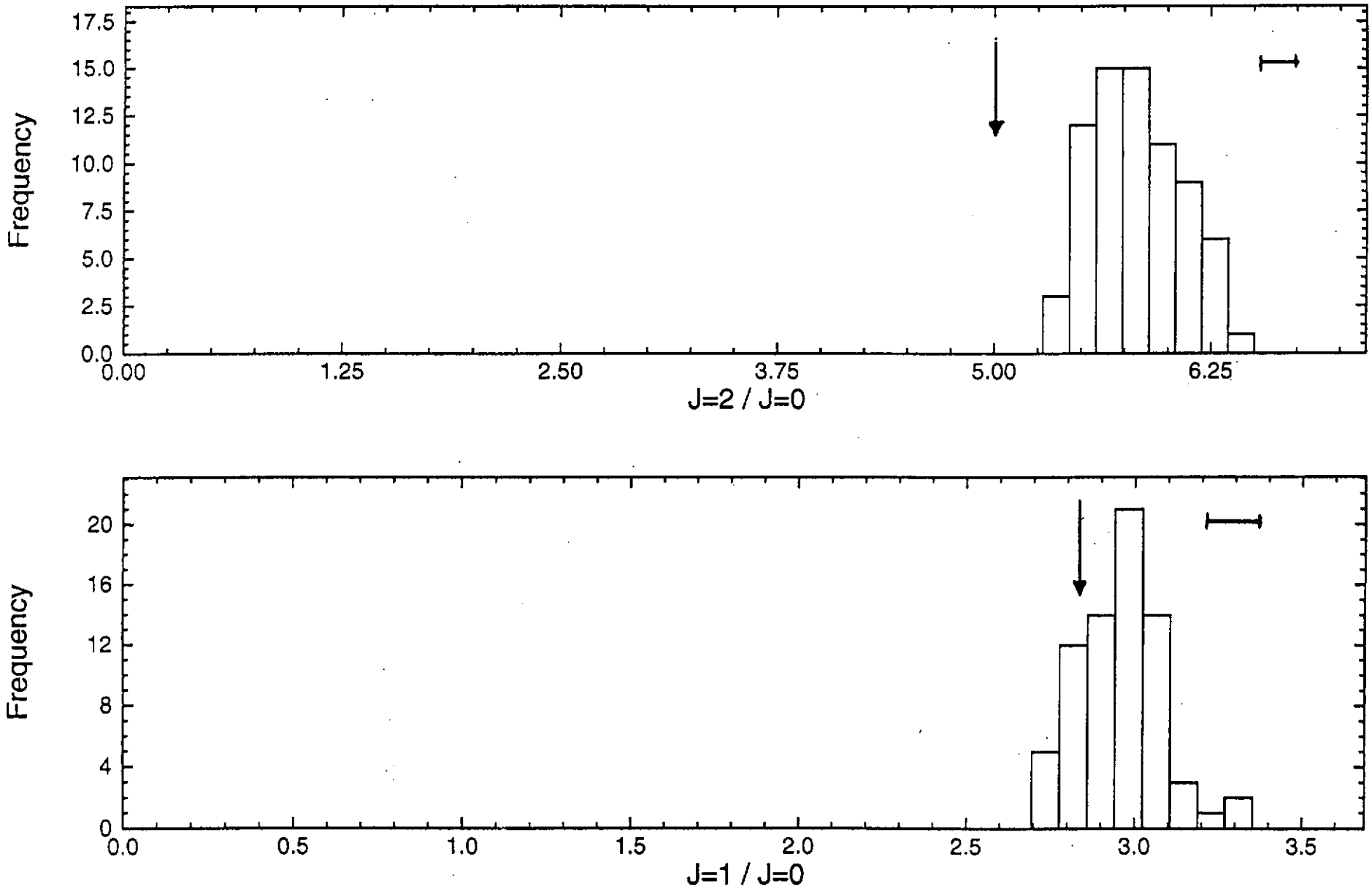
Frequency
17.5
15.0
12.5
10.0
7.5
5.0
2.5
0.0
0.00
1.25
2.50
3.75
5.00
6.25
J=2 / J=0
Frequency
20
16
12
8
4
0
0.0
0.5
1.0
1.5
2.0
2.5
3.0
3.5
J=1 / J=0

Fig.8

## Recent Issues of NIFS Series

NIFS-391 W.X.Wang, M. Okamoto, N. Nakajima, S. Murakami and N. Ohyabu,
*A Monte Carlo Simulation Model for the Steady-State Plasma in the Scrape-off Layer;* Dec. 1995

NIFS-392 Shao-ping Zhu, R. Horiuchi, T. Sato and The Complexity Simulation Group,
*Self-organization Process of a Magnetohydrodynamic Plasma in the Presence of Thermal Conduction;* Dec. 1995

NIFS-393 M. Ozaki, T. Sato, R. Horiuchi and the Complexity Simulation Group
*Electromagnetic Instability and Anomalous Resistivity in a Magnetic Neutral Sheet*; Dec. 1995

NIFS-394 K. Itoh, S.-I Itoh, M. Yagi and A. Fukuyama,
*Subcritical Excitation of Plasma Turbulence*; Jan. 1996

NIFS-395 H. Sugama and M. Okamoto, W. Horton and M. Wakatani,
*Transport Processes and Entropy Production in Toroidal Plasmas with Gyrokinetic Eletromagnetic Turbulence:* Jan. 1996

NIFS-396 T. Kato, T. Fujiwara and Y. Hanaoka,
*X-ray Spectral Analysis of Yohkoh BCS Data on Sep. 6 1992 Flares - Blue Shift Component and Ion Abundances -;* Feb. 1996

NIFS-397 H. Kuramoto, N. Hiraki, S. Moriyama, K. Toi, K. Sato, K. Narihara, A. Ejiri, T. Seki and JIPP T-IIU Group,
*Measurement of the Poloidal Magnetic Field Profile with High Time Resolution Zeeman Polarimeter in the JIPP T-IIU Tokamak*; Feb. 1996

NIFS-398 J.F. Wang, T. Amano, Y. Ogawa, N. Inoue,
*Simulation of Burning Plasma Dynamics in ITER*; Feb. 1996

NIFS-399 K. Itoh, S-I. Itoh, A. Fukuyama and M. Yagi,
*Theory of Self-Sustained Turbulence in Confined Plasmas*; Feb. 1996

NIFS-400 J. Uramoto,
*A Detection Method of Negative Pionlike Particles from a H2 Gas Descharge Plasma*; Feb. 1996

NIFS-401 K.Ida, J.Xu, K.N.Sato, H.Sakakita and JIPP TII-U group,
*Fast Charge Exchange Spectroscopy Using a Fabry-Perot Spectrometer in the JIPP TII-U Tokamak;* Feb. 1996

NIFS-402 T. Amano,
*Passive Shut-Down of ITER Plasma by Be Evaporation;* Feb. 1996

NIFS-403 K. Orito,

A New Variable Transformation Technique for the Nonlinear Drift Vortex; Feb. 1996

NIFS-404 T. Oike, K. Kitachi, S. Ohdachi, K. Toi, S. Sakakibara, S. Morita, T. Morisaki, H. Suzuki, S. Okamura, K. Matsuoka and CHS group; *Measurement of Magnetic Field Fluctuations near Plasma Edge with Movable Magnetic Probe Array in the CHS Heliotron/Torsatron*; Mar. 1996

NIFS-405 S.K. Guharay, K. Tsumori, M. Hamabe, Y. Takeiri, O. Kaneko, T. Kuroda, *Simple Emittance Measurement of H- Beams from a Large Plasma Source*; Mar. 1996

NIFS-406 M. Tanaka and D. Biskamp, *Symmetry-Breaking due to Parallel Electron Motion and Resultant Scaling in Collisionless Magnetic Reconnection*; Mar. 1996

NIFS-407 K. Kitachi, T. Oike, S. Ohdachi, K. Toi, R. Akiyama, A. Ejiri, Y. Hamada, H.Kuramoto, K. Narihara, T. Seki and JIPP T-IIU Group, *Measurement of Magnetic Field Fluctuations within Last Closed Flux Surface with Movable Magnetic Probe Array in the JIPP T-IIU Tokamak*; Mar. 1996

NIFS-408 K. Hirose, S. Saito and Yoshi.H. Ichikawa *Structure of Period-2 Step-1 Accelerator Island in Area Preserving Maps*; Mar. 1996

NIFS-409 G.Y.Yu, M. Okamoto, H. Sanuki, T. Amano, *Effect of Plasma Inertia on Vertical Displacement Instability in Tokamaks*; Mar. 1996

NIFS-410 T. Yamagishi, *Solution of Initial Value Problem of Gyro-Kinetic Equation*; Mar. 1996

NIFS-411 K. Ida and N. Nakajima, *Comparison of Parallel Viscosity with Neoclassical Theory*; Apr. 1996

NIFS-412 T. Ohkawa and H. Ohkawa, *Cuspher, A Combined Confinement System*; Apr. 1996

NIFS-413 Y. Nomura, Y.H. Ichikawa and A.T. Filippov, *Stochasticity in the Josephson Map*; Apr. 1996

NIFS-414 J. Uramoto, *Production Mechanism of Negative Pionlike Particles in $H_2$ Gas Discharge Plasma*; Apr. 1996

NIFS-415 A. Fujisawa, H. Iguchi, S. Lee, T.P. Crowley, Y. Hamada, S. Hidekuma, M. Kojima, *Active Trajectory Control for a Heavy Ion Beam Probe on the Compact*

*Helical System*; May 1996

NIFS-416 M. Iwase, K. Ohkubo, S. Kubo and H. Idei
*Band Rejection Filter for Measurement of Electron Cyclotron Emission during Electron Cyclotron Heating*; May 1996

NIFS-417 T. Yabe, H. Daido,T. Aoki, E. Matsunaga and K. Arisawa,
*Anomalous Crater Formation in Pulsed-Laser-Illuminated Aluminum Slab and Debris Distribution*; May 1996

NIFS-418 J. Uramoto,
*Extraction of $K^-$ Mesonlike Particles from a $D_2$ Gas Discharge Plasma in Magnetic Field;* May 1996

NIFS-419 J. Xu, K. Toi, H. Kuramoto, A. Nishizawa, J. Fujita, A. Ejiri, K. Narihara, T. Seki, H. Sakakita, K. Kawahata, K. Ida, K. Adachi, R. Akiyama, Y. Hamada, S. Hirokura, Y. Kawasumi, M. Kojima, I. Nomura, S. Ohdachi, K.N. Sato
*Measurement of Internal Magnetic Field with Motional Stark Polarimetry in Current Ramp-Up Experiments of JIPP T-IIU;* June 1996

NIFS-420 Y.N. Nejoh,
*Arbitrary Amplitude Ion-acoustic Waves in a Relativistic Electron-beam Plasma System*; July 1996

NIFS-421 K. Kondo, K. Ida, C. Christou, V.Yu.Sergeev, K.V.Khlopenkov, S.Sudo, F. Sano, H. Zushi, T. Mizuuchi, S. Besshou, H. Okada, K. Nagasaki, K. Sakamoto, Y. Kurimoto, H. Funaba, T. Hamada, T. Kinoshita, S. Kado, Y. Kanda, T. Okamoto, M. Wakatani and T. Obiki,
*Behavior of Pellet Injected Li Ions into Heliotron E Plasmas*; July 1996

NIFS-422 Y. Kondoh, M. Yamaguchi and K. Yokozuka,
*Simulations of Toroidal Current Drive without External Magnetic Helicity Injection;* July 1996

NIFS-423 Joong-San Koog,
*Development of an Imaging VUV Monochromator in Normal Incidence Region;* July 1996

NIFS-424 K. Orito,
*A New Technique Based on the Transformation of Variables for Nonlinear Drift and Rossby Vortices*; July 1996

NIFS-425 A. Fujisawa, H. Iguchi, S. Lee, T.P. Crowley, Y. Hamada, H. Sanuki, K. Itoh, S. Kubo, H. Idei, T. Minami, K. Tanaka, K. Ida, S. Nishimura, S. Hidekuma, M. Kojima, C. Takahashi, S. Okamura and K. Matsuoka,
*Direct Observation of Potential Profiles with a 200keV Heavy Ion Beam Probe and Evaluation of Loss Cone Structure in Toroidal Helical Plasmas on the Compact Helical System*; July 1996

NIFS-426 H. Kitauchi, K. Araki and S. Kida,
*Flow Structure of Thermal Convection in a Rotating Spherical Shell*; July 1996

NIFS-427 S. Kida and S. Goto,
*Lagrangian Direct-interaction Approximation for Homogeneous Isotropic Turbulence*; July 1996

NIFS-428 V.Yu. Sergeev, K.V. Khlopenkov, B.V. Kuteev, S. Sudo, K. Kondo, F. Sano, H. Zushi, H. Okada, S. Besshou, T. Mizuuchi, K. Nagasaki, Y. Kurimoto and T. Obiki,
*Recent Experiments on Li Pellet Injection into Heliotron E*; Aug. 1996

NIFS-429 N. Noda, V. Philipps and R. Neu,
*A Review of Recent Experiments on W and High Z Materials as Plasma-Facing Components in Magnetic Fusion Devices*; Aug. 1996

NIFS-430 R.L. Tobler, A. Nishimura and J. Yamamoto,
*Design-Relevant Mechanical Properties of 316-Type Stainless Steels for Superconducting Magnets*; Aug. 1996

NIFS-431 K. Tsuzuki, M. Natsir, N. Inoue, A. Sagara, N. Noda, O. Motojima, T. Mochizuki, T. Hino and T. Yamashina,
*Hydrogen Absorption Behavior into Boron Films by Glow Discharges in Hydrogen and Helium*; Aug. 1996

NIFS-432 T.-H. Watanabe, T. Sato and T. Hayashi,
*Magnetohydrodynamic Simulation on Co- and Counter-helicity Merging of Spheromaks and Driven Magnetic Reconnection*; Aug. 1996

NIFS-433 R. Horiuchi and T. Sato,
*Particle Simulation Study of Collisionless Driven Reconnection in a Sheared Magnetic Field*; Aug. 1996

NIFS-434 Y. Suzuki, K. Kusano and K. Nishikawa,
*Three-Dimensional Simulation Study of the Magnetohydrodynamic Relaxation Process in the Solar Corona. II.*; Aug. 1996

NIFS-435 H. Sugama and W. Horton,
*Transport Processes and Entropy Production in Toroidally Rotating Plasmas with Electrostatic Turbulence*; Aug. 1996

NIFS-436 T. Kato, E. Rachlew-Källne, P. Hörling and K.-D Zastrow,
*Observations and Modelling of Line Intensity Ratios of OV Multiplet Lines for 2s3s 3S1 - 2s3p 3Pj*; Aug. 1996